Energy and Environmental Systems Group
Institute for Sustainable Energy, Environment and Economy (ISEEE)

Geomechanical Modelling and Analysis

Wabamun Area CO_2 Sequestration Project (WASP)

Authors

Somayeh Goodarzi

Dr. Antonin (Tony) Settari

Rev.	Date	Description	Prepared by
1	September, 2009	Geomechanical Modelling and Analysis	Somayeh Goodarzi Dr. Antonin (Tony) Settari

Table of Contents

List of Tables

List of Figures

BACKGROUND

Large stationary CO_2 emitters are located in central Alberta with cumulative annual emissions in the order of 30 Mt CO_2. This includes four coal-fired power plants in the Wabamun Lake area, southwest of Edmonton with emissions between 3 and 6 Mt/year. Although significant CO_2 storage capacity exists in depleted oil and gas reservoirs in this area, these may not be available in the near future because most of these reservoirs in the Wabamun lake area are still producing. Moreover, the large Pembina Cardium oil fields, located just south of the Wabamun Lake area, now producing as mature waterfloods, are in the initial stages of investigating possible use of CO_2 as a miscible flooding agent to further enhance oil recovery. Commercial scale use of CO_2 for this purpose is still a few years away and until then these pools will require only pilot scale volumes of CO_2 for EOR reservoir characterization and test purposes. As a result, CO_2 storage in deep saline aquifers is the most likely near future scenario for large scale CO_2 sequestration. While it is certainly possible to move CO_2 from the Wabamun area to distant storage locations, it is of considerable interest to public policy makers to determine if very large scale storage is feasible in the immediate vicinity of the power plants.

The study will perform a comprehensive characterization of large-scale CO_2 storage opportunities in the Wabamun Lake area and to analyze any potential risks. As a benchmark, the project will examine the feasibility of storing 20 Mt-CO_2/year for 50 years within a study area of 60 km by 90 km in the Wabamun area. This Gigaton-scale storage project is one to two orders of magnitude larger than the commercial projects now under study. It will fill a gap between the province-wide capacity estimates (which do not involve site specific studies of flow and geomechanics, etc.) and the detailed commercial studies of small CO_2 storage projects currently underway. Unlike the commercial projects, this study has been conducted as a public non-confidential project lead by the University of Calgary (Keith *and Lavoie*, 2008).

1. INTRODUCTION

Based on current sequestration pilot projects and enhanced oil recovery efforts, evidence suggests that geologic sequestration is a technically viable means to significantly reduce anthropogenic emissions of CO_2. One of the most important concerns with respect to the long term CO_2 storage is that stress changes caused by injection could lead to the formation or reactivation of fracture networks and fault movements which could potentially provide pathways for CO_2 migration through previously impermeable rocks (Quintessa et al., 2007). A portion of injected CO_2 can escape the storage domain if the integrity of the seal rock is violated by geomechanical mechanisms such as fault reactivation, propagation of induced fractures or rock shear failure. In order to determine whether the stress state compromises the ability of the formation to act as an effective storage unit, a geomechanical assessment of the formation integrity must be carried out, by the means of coupled flow and geomechanical modelling. In recent decades there has been significant effort towards developing simulation techniques to model the aforementioned mechanisms for petroleum industry applications. The goal of this study is to further develop this simulation technology and modelling tools to model and understand the mechanisms and physics of the geomechanical effects occurring during or after CO_2 injection.

2. OBJECTIVES

The purpose of this report is to study the geomechanical effects of CO_2 injection in the Nisku aquifer located in Wabamun Lake area. The study utilized GEOSIM, a fully coupled reservoir flow and geomechanical model. GEOSIM is a commercial code of TAURUS Reservoir Solutions Ltd., which is available for research at University of Calgary under academic license.

The following major objectives are addressed in this report.

1. Study the stress variation and displacement pattern.
2. Examine the possibility of shear failure in reservoir and caprock layer.
3. Investigate the possibility of increasing well injectivity by injection at fracturing pressure, study fracture propagation and evaluate the risk of fracturing the caprock.
4. Incorporate thermal effects in the geomechanical model and determine the effects of cooling due to injection on stresses, displacements and fracture propagation.
5. Investigate the benefit of using production wells to crossflow to other zones in order to reduce average pressure increase.

The results can be then used, in conjunction with other work done in the WASP feasibility study, to define the optimum injection scenario in terms of technical and economical feasibility of the WASP project. In particular, the injection at fracturing conditions (i.e., propagating dynamic fracture during injection) and the use of production wells are novel ideas for increasing the efficiency of CCS.

3. THE WASP MODEL

3.1. Model Geometry

The model geometry and reservoir characterization was derived from the flow model built in reservoir simulation sub-task of the WASP study. Figure 1 shows the pressure distribution after 50 years of injection in the Nisku aquifer. Since the pressure plume is not extended to the north side of the aquifer and because the geomechanical effects strongly depend on pressure variation, the north side of the aquifer is not included in this study. The geomechanical model, which only included the area inside the red dashed rectangle (Figure 1), was superimposed on the updated flow model. The areal extent of the flow and geomechanical models is the same but the geo-model is extended in the vertical direction to model the caprock and the shallow layers up to the surface. The areal size of both models is 338,100 × 119,340 (m) and the vertical thickness of the flow and geo-model are 70 (m) and 1930 (m) respectively. The flow and geomechanical models consist of $97 \times 62 \times 4 = 24056$ and $97 \times 62 \times 9 = 54{,}126$ grid blocks, respectively. The reservoir is represented by 4 layers, with the smallest layer at the top, in order to capture the CO_2 plume override. A detailed CO_2 placement study carried out in the reservoir simulation subtask of the WASP study shows that even more layers are required for high accuracy, but finer models were not possible at this stage due to very large computer requirements of the coupled model.

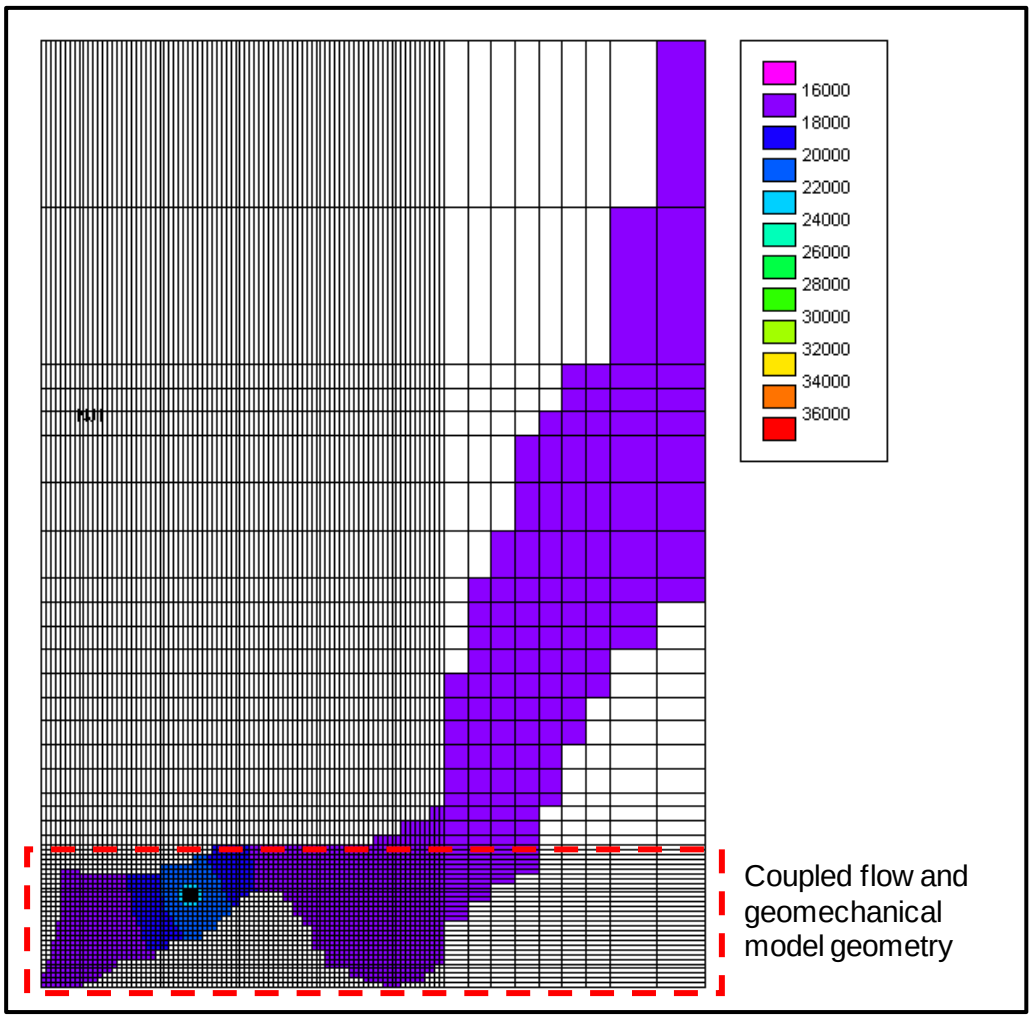

Figure 1: Plan-view of the pressure (kPa) distribution at the middle of Nisku aquifer after 50 years of injection.

3.2. The Flow Model

The water-gas relative permeability functions for the Nisku carbonate aquifer are derived from the experimental data published by Bennion and Bachu (2005) and are shown in Figure 2.

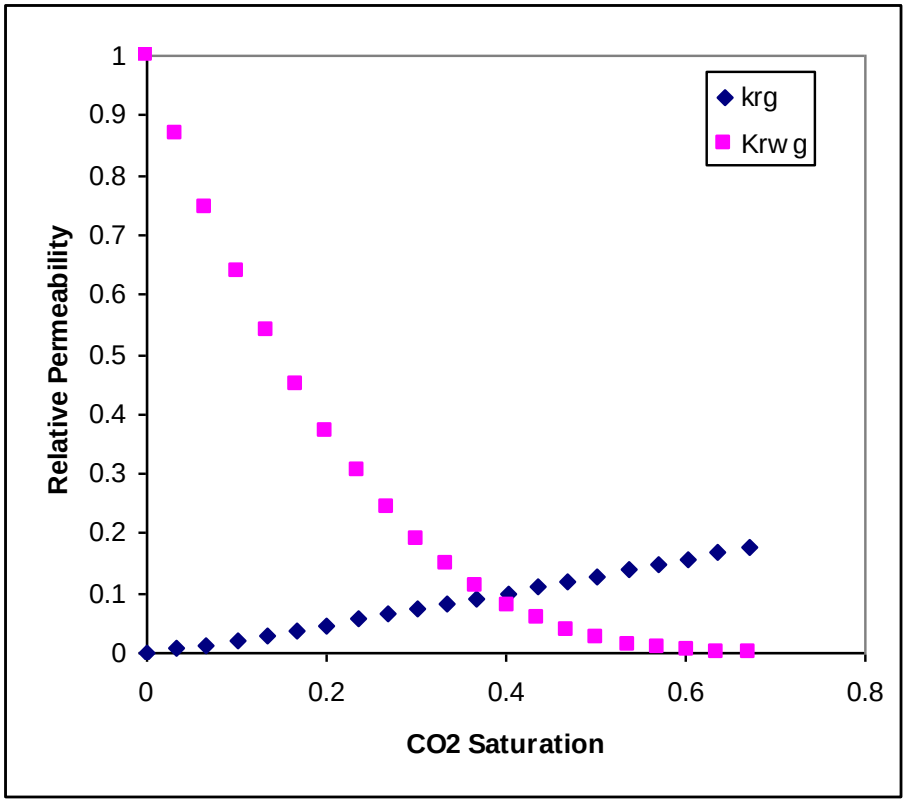

Figure 2: Brine-CO_2 relative permeability curves for Nisku carbonate aquifer (from Bennion and Bachu, 2005).

The PVT model is generated using the method developed by Hassanzadeh et al. (2007), which creates 2-component black oil PVT data for densities, solubility of CO_2 and viscosities. To generate the Nisku PVT data, formation temperature and water salinity level are estimated at 60 C and 190,000 ppm respectively (Hitchon, 1996). The PVT input data for the GEOSIM model is shown in Figures 3, 4 and 5.

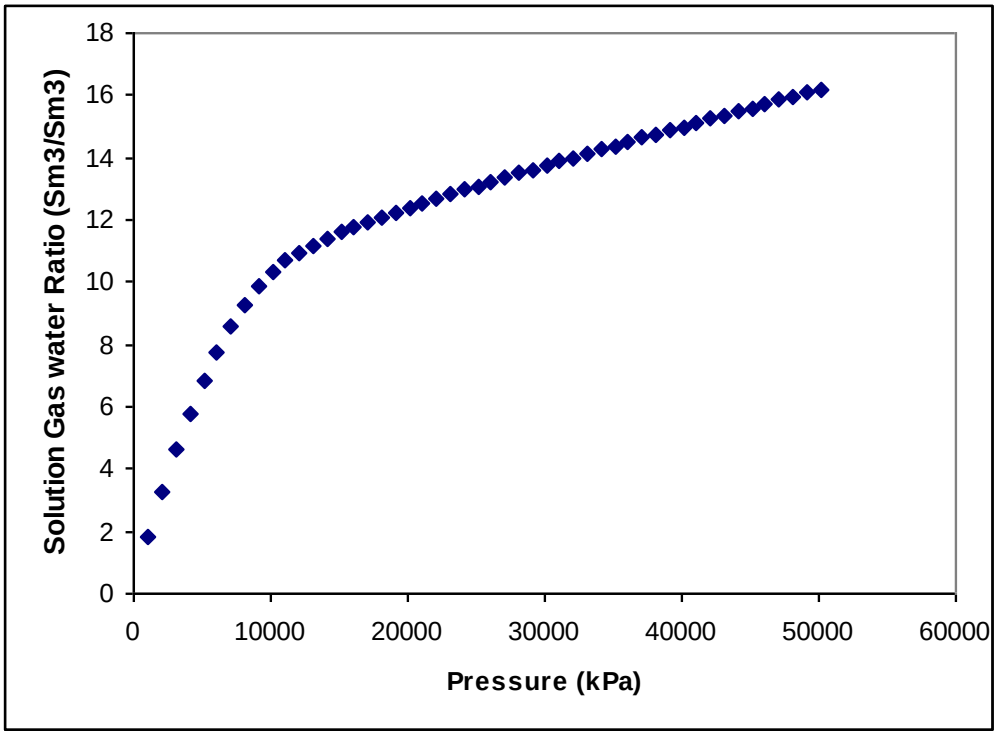

Figure 3: Solution Gas (CO_2) Water Ratio for Nisku carbonate aquifer.

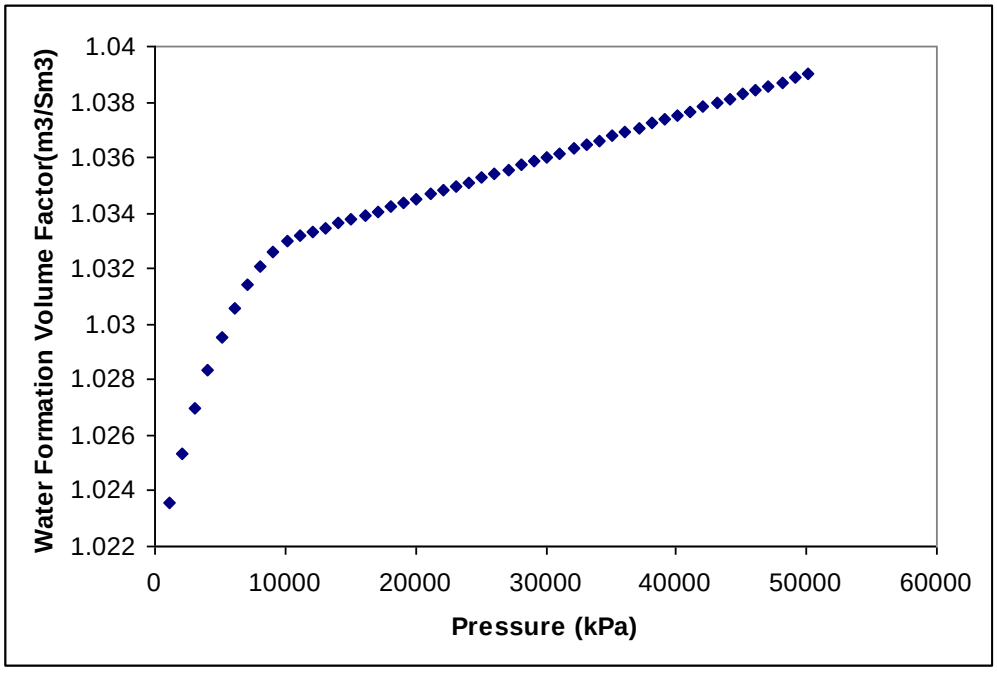

Figure 4: CO_2 saturated Water Formation Volume Factor for Nisku carbonate aquifer.

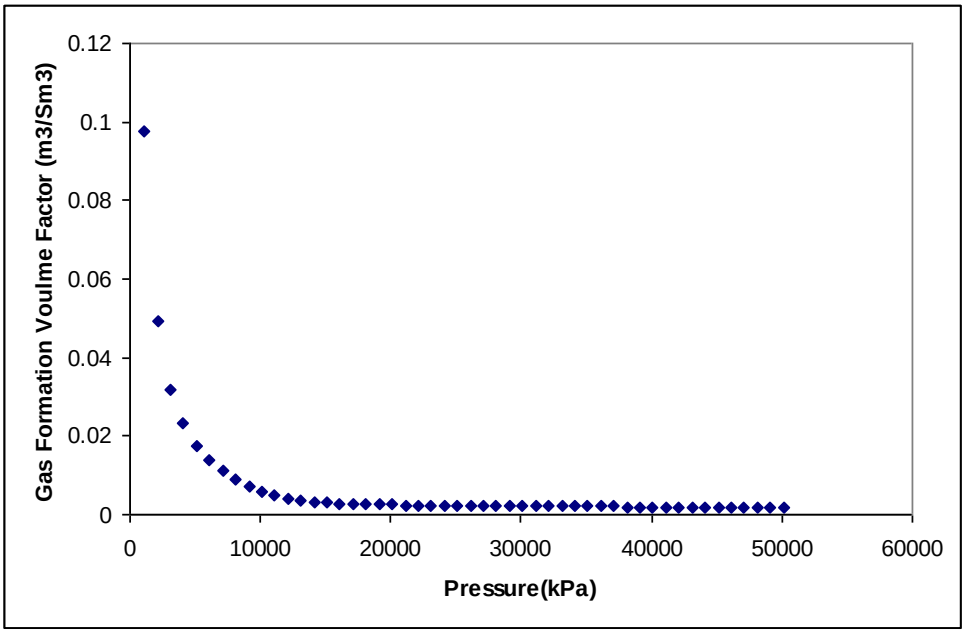

Figure 5: CO_2 Formation Volume Factor.

3.3. Geomechanical Properties

Geomechanical properties were available for the Nisku aquifer and the overlying geological layers up to 1200 m depth. Since the geomechanical input data were not provided for shallow layers with less than 1200 m depth, the remaining overburden was modelled as one layer. Its properties were obtained by extending the given properties of the topmost layer. Table 1 lists the input rock mechanical properties used for the target zone and the layers above it.

The initial distribution of stresses was assumed to have constant gradients for the S_{Hmax} (maximum horizontal stress), S_{hmin} (minimum horizontal stress) and S_v (vertical stress) and is shown in Figure 6 (Michael et. al., 2008). The pore pressure gradient was considered equal to fresh water hydrostatic gradient. The maximum stress gradient was approximated to be in the range of 20-23 kPa/m. Due to normal faulting regime in Wabamun lake area, the maximum stress was assumed to be equal to the vertical stress. The direction of S_{hmin} was approximately 145°, in a general southeast-northwest direction (Bell and Bachu). The stress directions are shown in Figure 7. Because of the lack of more detailed stress-strain data, linear elasticity was assumed in the simulation, with the parameters from Table 1.

The data in Table 1 have been provided by the Geomechanical Characterization group of the WASP team. The corresponding derivation method can be found in section 3 of this team's report. The mechanical properties were kept constant for each geological layer and layers with similar geological and geomechanical properties were lumped together. Therefore more spatial refinement is required in order to accurately represent the local rock properties and stress profile at particular well locations.

Table 1: Input rock mechanical properties.

Layers	Thickness (m)	Young's Modulus (kPa)	Poisson's Ratio	Thermal Expansion Coefficient (1/oC)	Grain Modulus (kPa)	Bulk Density (Kg/m^3)
Shale, surface-Joli Fou	1173.3	2.16E+07	0.32	1.51E-05	6.00E+07	2500
Sandstone, Ellerslie-Manville	167.7	3.17E+07	0.29	1.79E-05	7.00E+07	2500
Carbonate, Wabamun-Nordegg	476.6	6.52E+07	0.26	1.50E-05	8.00E+07	2500
Shale, Calmar	42.4	7.53E+07	0.28	1.76E-05	6.00E+07	2500
Carbonate, Nisku	70	6.15E+07	0.29	1.50E-05	8.00E+07	2500

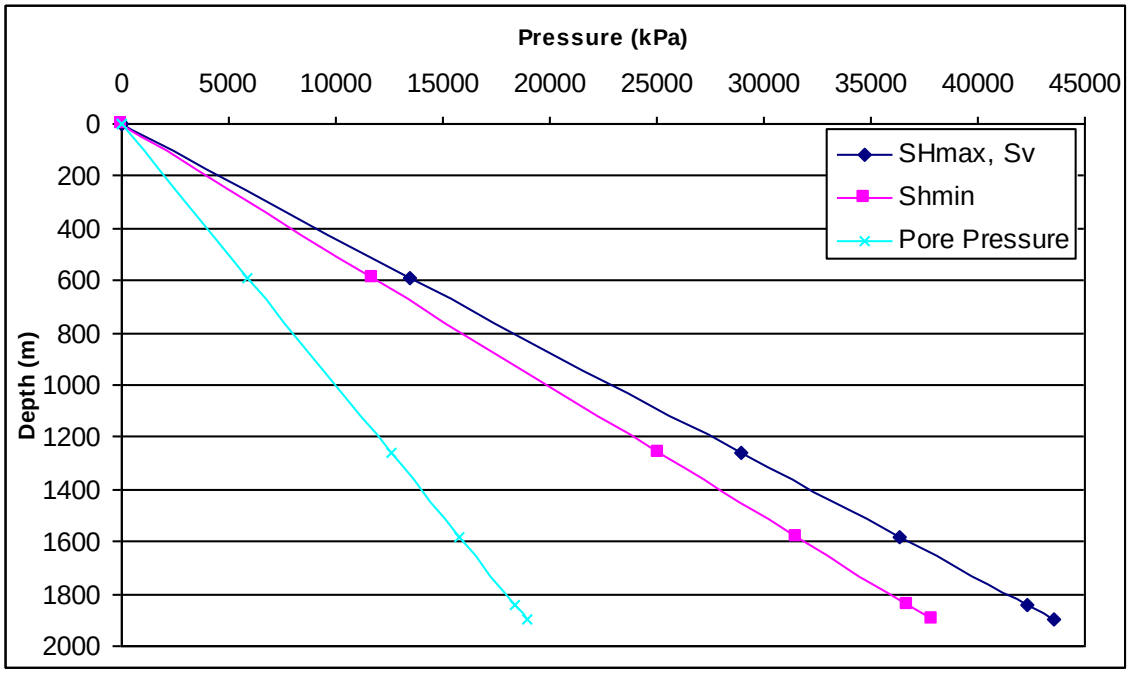

Figure 6: Stress profile from Alberta Geological Survey database.

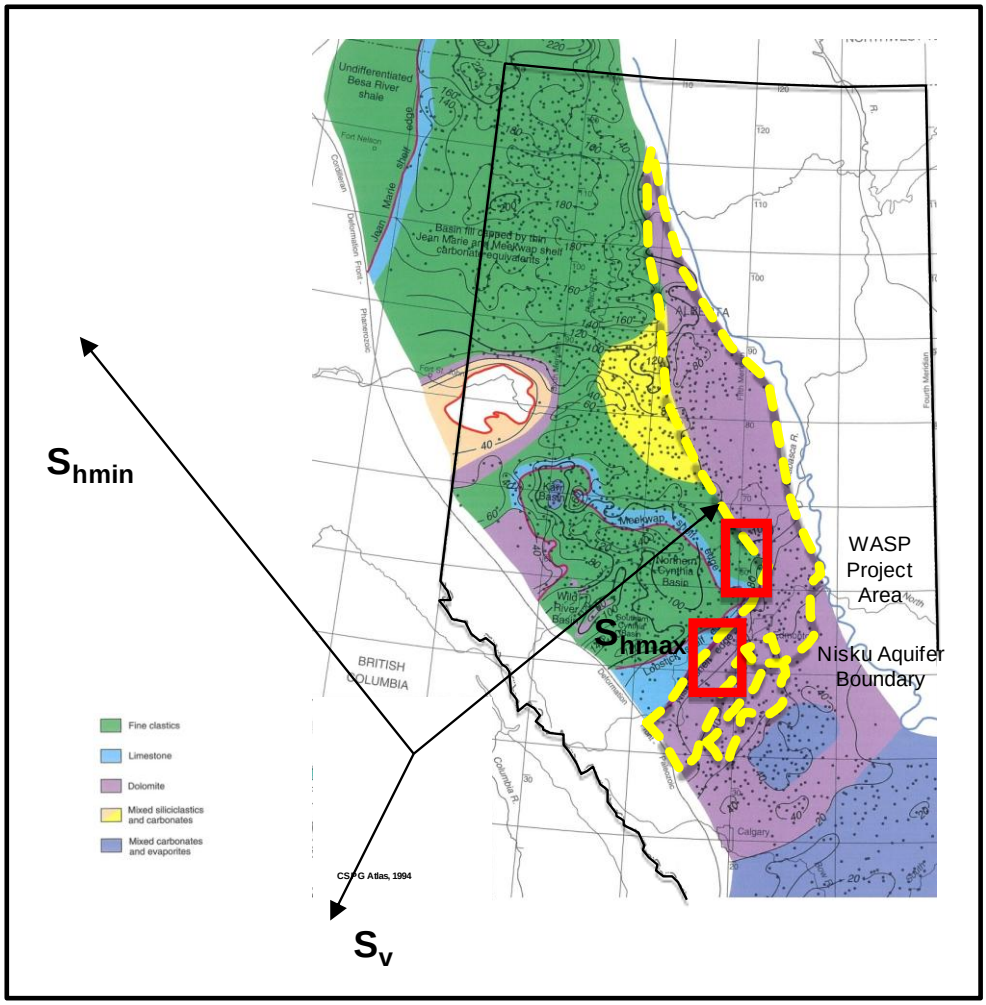

Figure 7: Lithology and principal stress directions in Wabamun area. The yellow dotted boundary line shown on this diagram illustrates the edges of the porous and permeable regions of the Nisku Aquifer. The red box is the WASP project region (Mossop and Shetsen).

4. RESULTS—ISOTHERMAL INJECTION WITHOUT CONSIDERATION OF FRACTURING

The first set of results presented is for the case when the injection pressure is limited by assumed fracturing pressure of 40 MPa and fracture propagation is not considered. The well in those models was injecting at a rate of 1 Mton/yr (=51,362 MScf/day). The limiting pressure was the same as in the work of the WASP group doing uncoupled flow modelling, to provide consistency between the results, and the reasoning for the choice of this value is presented elsewhere.

All the results in this Section are obtained using isothermal modelling (i.e., the injected CO_2 temperature equal to reservoir temperature). In Section 6 we will examine the effect of injecting cooler CO_2 which will dramatically affect the fracturing pressure.

4.1. Stress Changes and Displacement Pattern

As expected, after CO_2 has been injected in the Nisku aquifer, the formation will undergo deformations in all directions in order to place the injected volume. In this section the displacements in three different directions are presented.

At the end of injection, the maximum vertical displacement will reach ~4 mm at reservoir's topmost layer. As one travels from reservoir's topmost layer to the surface the value of the vertical displacement will decrease to ~2 mm. The extent of this decay in deformation depends on the mechanical properties of the overburden. The vertical displacement at the surface after 50 years of injection is shown in Figure 8. The magnitudes of displacements after this long-time injection are small and on the order of 1 millimetre.

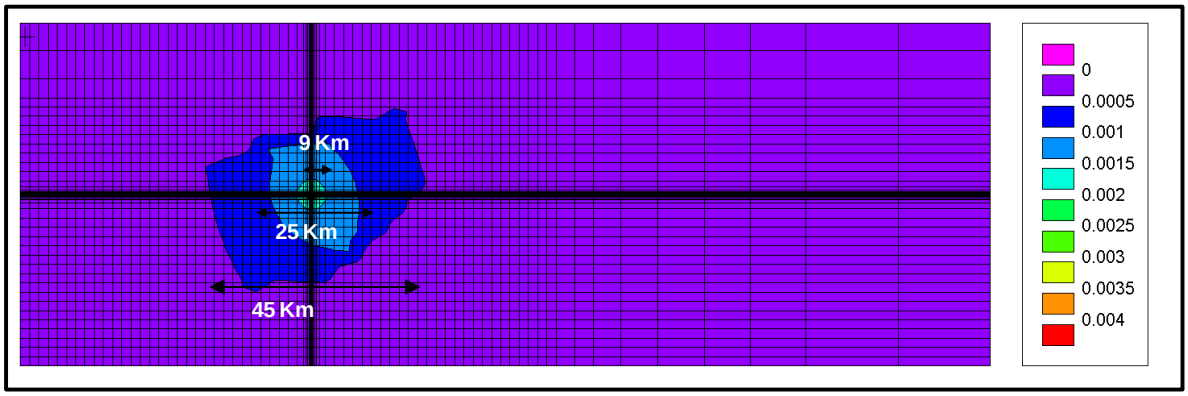

Figure 8: Vertical Displacement (metre) at ground surface after 50 years of injection at 1Mton/yr below fracture pressure.

The horizontal displacements of the reservoir layer are shown in Figures 9 and 10. Since the model is not symmetric around the wellbore in the x-direction, the horizontal displacement in this direction is not symmetric. However in y direction since the two boundaries has roughly the same distance to the wellbore, a symmetric pattern is observed.

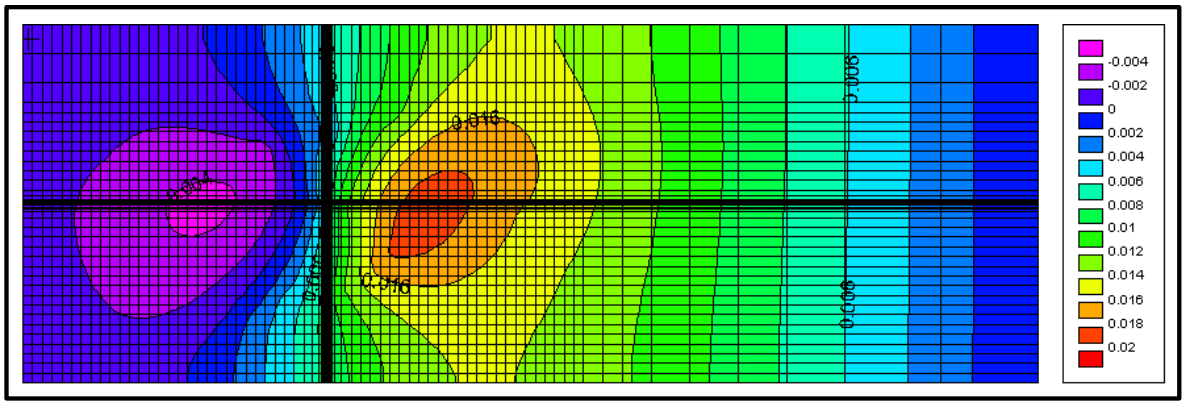

Figure 9: X-Direction Displacement (metre) at Reservoir's top layer after 50 years of injection at 1Mton/yr below fracture pressure (see Figure 7 for orientations of the x and y directions).

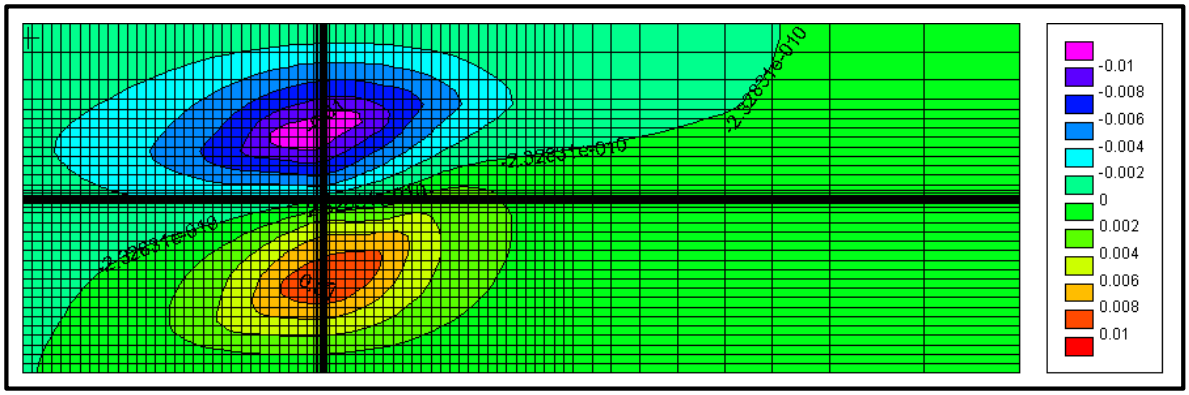

Figure 10: Y-Direction Displacement (metre) at Reservoir's top layer after 50 years of injection at 1Mton/yr below fracture pressure.

The results presented are preliminary and are based on the input mechanical properties and stresses as discussed in Section 3. The displacements are an important result of the simulation because they can be matched to the uplift, tiltmeter and other data and also be used for planning the location of instrumentation and improving the quality of input rock mechanical properties.

Also since the downhole tiltmeter measurements can identify where the pressure plume is, surface displacement measurements could be utilized to validate the flow model and determine the extent of pressure plume.

The measured magnitude of the deformations (vertical uplift) can be used to confirm system compressibility in the injection zone (important for injectivity) and possibly mechanical properties of the overburden.

4.2. Stress variation with pore pressure changes

The area around the well will gradually pressure up during the injection period. In order to study the effect of increased pore pressure on total stresses and to confirm the 1-D consolidation theory, the well block in Nisku's middle layer is considered for analysis. Figure 11 shows the horizontal stress variation with pressure for the well grid block in Nisku.

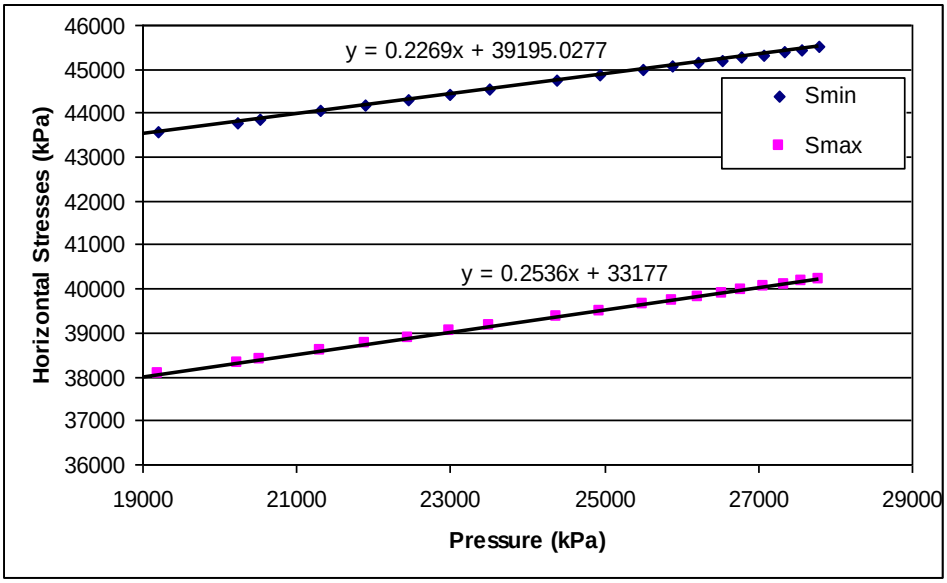

Figure 11: Variation of horizontal stresses versus pressure. x and y in the regression equations represents the pressure and horizontal stresses respectively.

As pore pressure is increasing, small variations in all stresses are observed. If it is assumed that the behavior of the rock is following the 1-D consolidation theory, then the horizontal stresses will change with the average reservoir pressure *P* according to the following equation:

$$S_h = S_v \frac{\nu}{1-\nu} + \alpha P \frac{1-2\nu}{1-\nu} = S_{hi} + \eta P$$

$$\alpha = 1 - \frac{C_s}{C_b} = 1 - \frac{K_b}{K_s}$$

Where,

S_h is the horizontal stress.
S_v is the vertical stress.
ν is the Poisson ratio.
α is the Biot's constant.
C_s is the grain compressibility.
C_b is the bulk compressibility.
K_b is the rock's bulk modulus.
K_s is the rock's grain modulus .
P is the pressure.

The Biot's constant for Nisku was calculated from the input geomechanical properties as 0.39 and then η was determined from the following equation.

$$\eta = \alpha \frac{1-2\upsilon}{1-\upsilon} = 0.2307$$

Then the slope of S_h versus P in Figure 10 should be equal to η. For our data, $\eta = 0.2307$ which agrees with the simulation data. This means that the deformation around the injector is close to uniaxial.

4.3. Shear Failure

As it is well known, it is possible for a formation to reach shear failure even before exceeding fracture pressure. Figure 12 shows the concept of the Mohr Coulomb criteria for shear failure. When the magnitude of shear stress exceeds the shear strength of the rock, the state of stress will exceed the failure envelope of the Mohr Coulomb diagram and shear failure will happen.

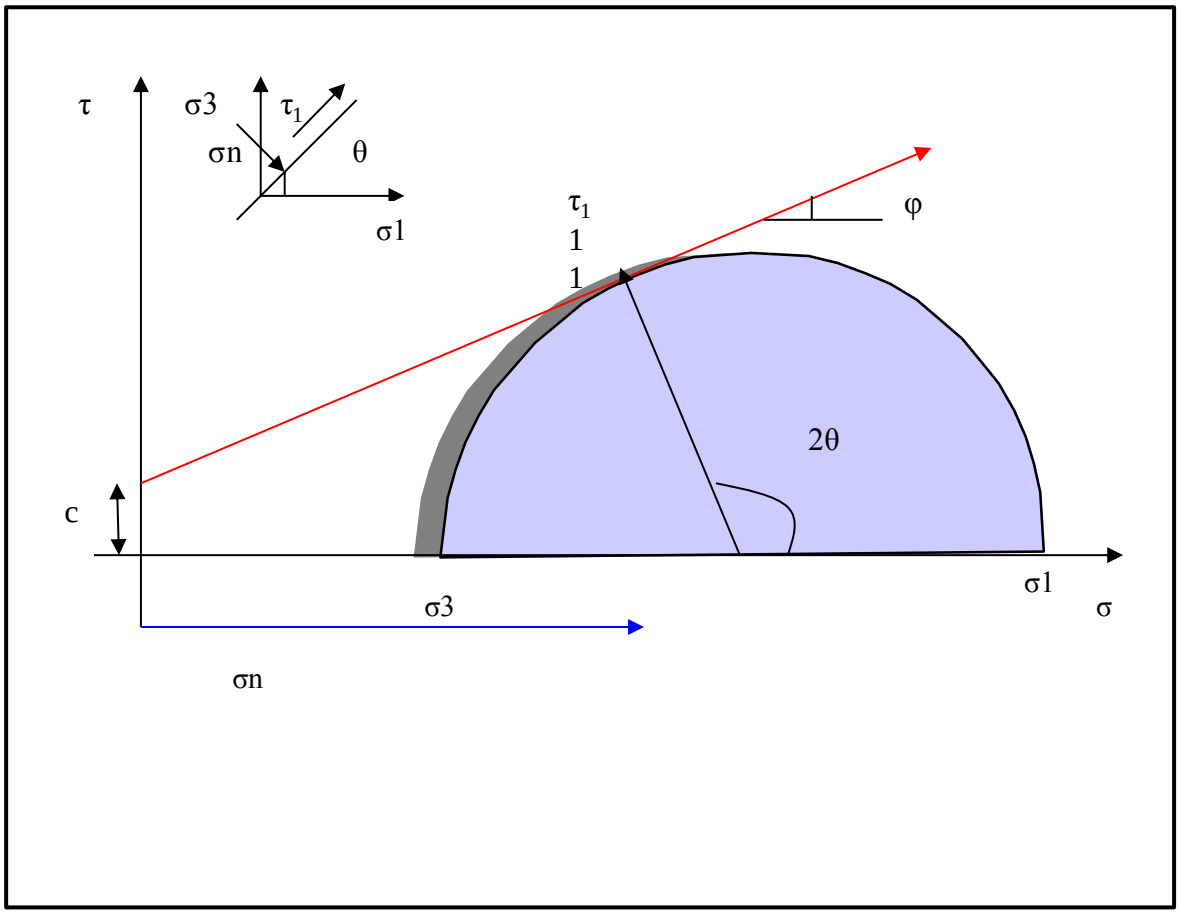

Figure 12: Mohr Coulomb Diagram.

The failure envelope of Mohr-Coulomb is defined by the following formula.

$$\tau = c + \tan(\varphi)\sigma$$

Where,

τ is the shear stress.
c is Cohesion.
φ is friction angle.
σ is normal stress.

In order to determine how close this formation is to shear failure, the concept of stress level is introduced here. Stress level is defined as the ratio of deviatoric stress at the current condition to the deviatoric stress at failure condition and is presented by the following equation:

$$l_\sigma = \frac{\sigma'_{dev}}{(\sigma'_{dev})_f} \leq 1 \qquad \sigma'_{dev} = \sigma'_{\max} - \sigma'_{\min}$$

Where,

l_σ is the stress level.
σ'_{dev} is the deviatoric stress at the current condition.
$(\sigma'_{dev})_f$ is the deviatoric stress at failure.
$\sigma'_{\max}$ is the maximum principal stress.
$\sigma'_{\min}$ is the minimum principal stress.

The deviatoric stress at failure is a function of cohesion c and friction angle φ according to:

$$(\sigma'_{dev})_f = \frac{2cCos\phi + 2\sigma'_3 Sin\phi}{(1 - Sin\phi)}$$

When the stress level is less than 1, the shear stress has not exceeded the shear strength of the rock and when it exceeds 1, the shear strength of the rock has been reached in a plane which is aligned in the direction found from the Mohr Coulomb circle. The cohesion and friction angle used in this study are listed in Table 2. The friction angle is assumed to be constant and equal to 30 for all layers since it has been suggested that it is a good rough estimate for this value (Zoback, 2007). Cohesion was calculated from the following correlation given the friction angle and provided unconfined compressive strength.

$$UCS = 2c\frac{Cos\varphi}{1 - Sin\varphi}$$

Where,

UCS is unconfined compressive strength.
c is cohesion.
φ is friction angle.

Figure 13 shows stress level values in the formation after 50 years of injection. These values are all significantly less than one which implies that this formation is not in danger of shear failure under this scenario.

Table 2: Cohesion and friction angle for geomechanical model.

Layers	Thickness(m)	Cohesion(MPa)	Friction angle (Deg)
Shale, surface-Joli Fou	1173.3	8.97	30
Sandstone, Ellerslie-Manville	167.7	12.55	30
Carbonate, Wabamun-Nordegg	476.6	27.79	30
Shale, Calmar	42.4	32.31	30
Carbonate,Nisku	70	40.41	30

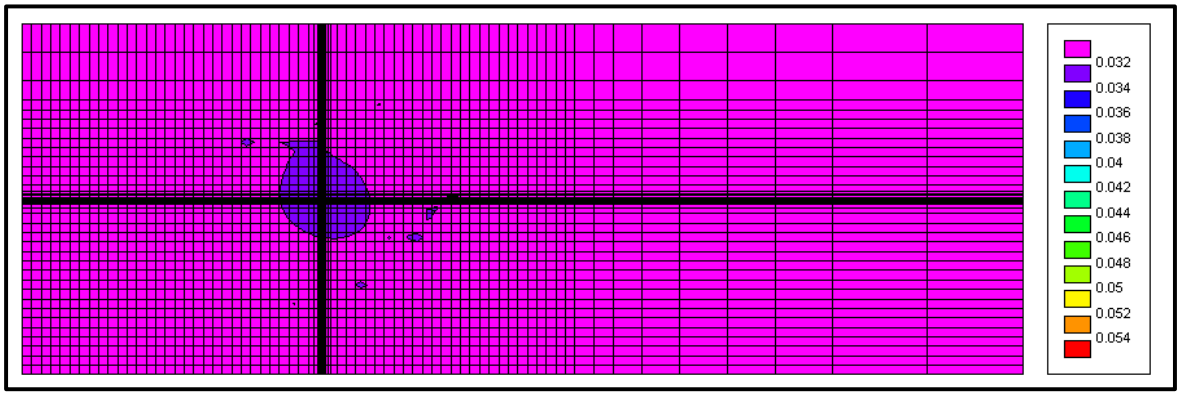

Figure 13: Stress level at Nisku's middle layer after 50 years of injection of 1Mton/yr below fracture pressure. Stress level which shows the closeness of the formation rock to shear failure, varies between 0 and 1.

Figure 14 shows the stress state of Nisku layer inside the Mohr Coulomb at the beginning of injection and after 50 years. Once the pressure increases in the reservoir, which helps reduce the effective stress, the Mohr Coulomb circle moves to the left. If the circle touches the Mohr criterion which is shown by the red line in Figure 14, the rock fails in shear. As it is observed, the Nisku aquifer is not likely to experience shear failure. This is due to the large value of cohesion used (40 Mpa) and relatively small differences in the initial principal stresses.

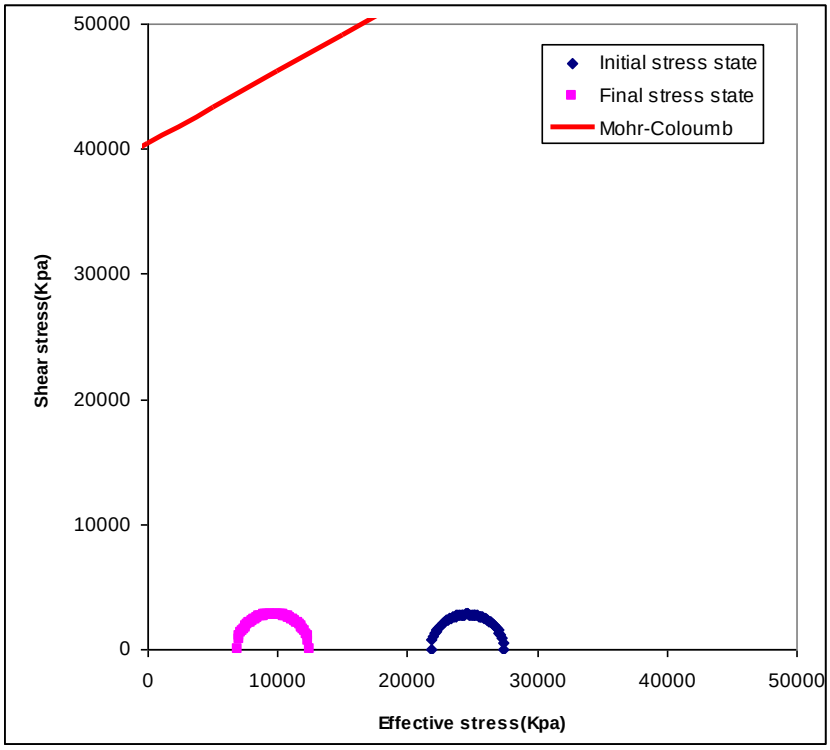

Figure 14: Mohr Coloumb Criteria for Nisku aquifer layer.

4.4. Sensitivity Analysis

Since the friction angle of the rock mass can be assumed to be constant at 30 Deg (Zoback, 2007), a sensitivity analysis has been carried out on the cohesion value. Cohesion of the intact carbonate rock is high, but the effective value can be much lower due to the presence of natural fractures and other heterogeneities. As expected when the cohesion value of the rock decreases, the likelihood of shear failure grows. This is illustrated in Figure 15, where the same simulation was run with different cohesion values. As c decreases, the stress level in the well block increases significantly. However shear failure is not reached even at zero cohesion (i.e., stress level=1), due to small difference between the maximum and minimum stress. Given the uncertainty of other data, there could be some failure if the effective cohesion is very low.

Another consideration is the friction angle of the interface between the Nisku and the shale (if such interface exists). For example, thin clay layers can have much lower cohesion, as well as friction angle. Failure would then happen along the interface, and this mechanism would stop fracture vertical growth.

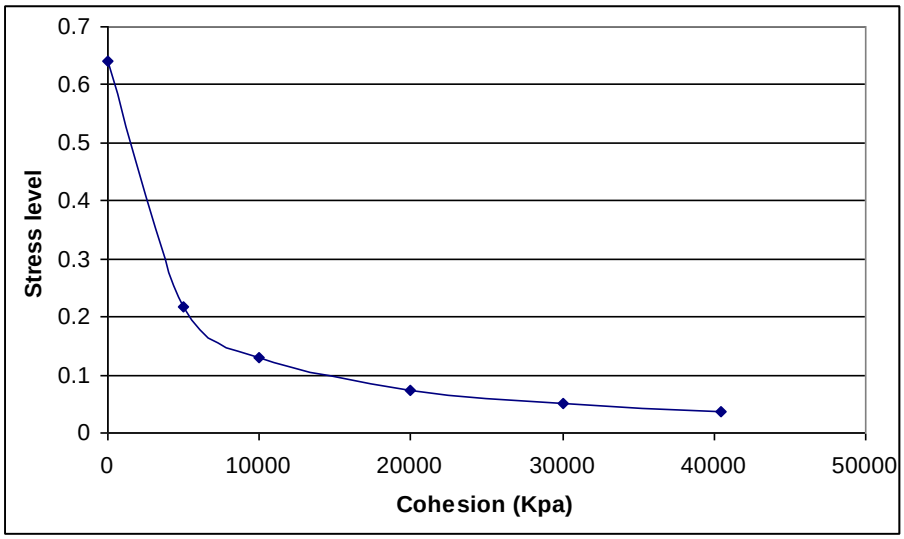

Figure 15: Sensitivity analysis for rock cohesion value—stress level at the wellbore as a function of rock cohesion.

5. RESULTS—ISOTHERMAL INJECTION CONSIDERING FORMATION FRACTURING

Allowing dynamic fracturing (by removing the BHIP restriction) has the potential for increasing the well injectivity. However it is important to model (and monitor in the actual operation) the fracture growth for several reasons:

- To make sure fracture would not propagate through the caprock to the extent that it would create a loss of containment (i.e., connect to other permeable zone)
- To use the information on fracture length to design correctly the well pattern
- To be able to control the injection rates to avoid excessive fracture lengths

The results presented here are the first preliminary work in this area, which demonstrates the concepts of the modelling and feasibility of the process. More detailed work would be required to arrive at reliable fracture growth predictions that could be used to design the injection scheme. Such work should be supported by field pilot data and lab geomechanical data.

5.1. Modelling Fracture Propagation

It is important to model the fracture growth both laterally and vertically to make sure it would not propagate through the caprock and reach other potential loss zones. To do that, the caprock layers were included in the flow model to track the possible fracture growth through them. A small porosity of 0.01, horizontal and vertical permeability of 3×10^{-5} md and 3×10^{-7} md were assigned to the caprock layers. Then the fracture was allowed to propagate both in the Nisku zone and in the layers above, using the numerical techniques described below. Since the minimum stress is in the y direction, the induced fracture plan would be perpendicular to this direction. Figure 16 shows the stress direction along with the induced fracture plane. This figure shows a section which is cut from the full geomechanical model and the well is located at the front corner of this element. Blue and yellow layers in this picture show the reservoir and shale layers respectively.

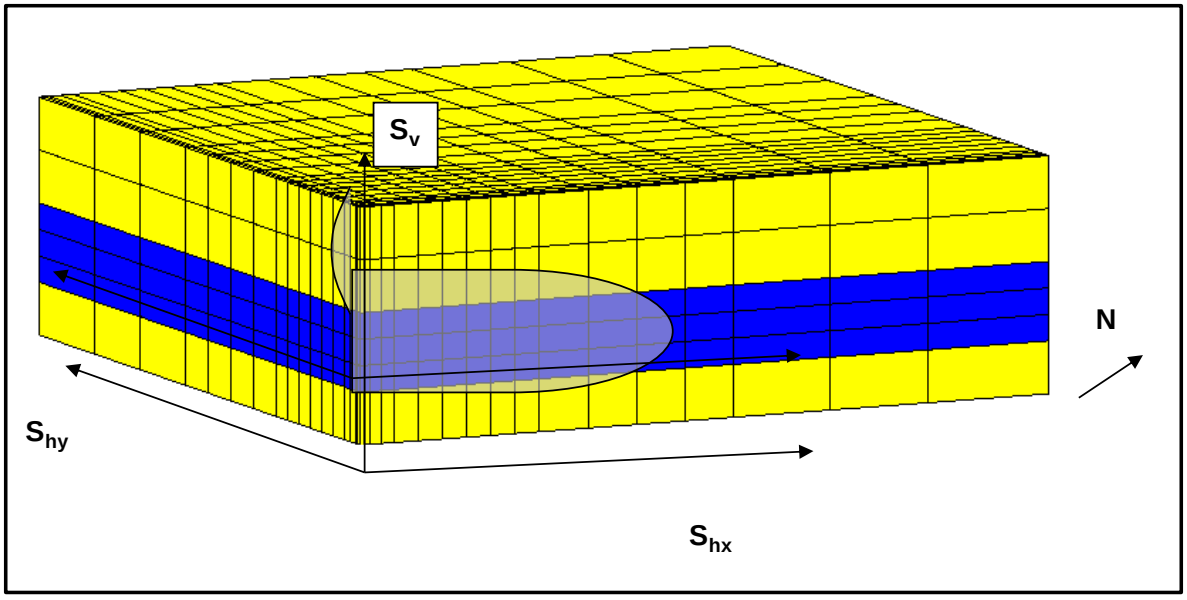

Figure 16: Induced fracture plane.

5.1.1 Transmissibility multipliers

In order to model the dynamic fracture propagation, a transmissibility multiplier table is incorporated in the model. All entries are calculated based on the estimation of fracture opening of Griffith fracture model as follows:

$$TMULT = \frac{K_m A_m + K_f A_f}{K_m A_m} = 1 + \frac{w^3{}_f}{12 K_m w}$$

$$w_f = \frac{\Delta PL}{\overline{E}} = \frac{\Delta PL * 4(1-\upsilon^2)}{E}$$

Where,

TMULT is the transmissibility multiplier.
K is permeability.
A is the cross section area for fluid flow.
W_f is the fracture spacing.
W is the fracture thickness.
ΔP is a representative value of net pressure or effective stress on the rock.
L is the fracture half-height (based on the 2-D Perkins-Kern geometry assumption of vertical fracture with smooth closure at the top and bottom) (Perkins and Kern, 1961)
E is the Young's Modulus of the formation rock.
ν is the Poisson's ratio of the formation rock.
Subscript m refers to matrix property
Subscript f refers to fracture property

The Transmissibility Multiplier table can be incorporated in the model both as a function of pressure or effective minimum stress. In order to calculate the multiplier, a fracture half height of

35 m (equal to half-height of the Nisku aquifer) is considered and the rest of the data are taken from the mechanical properties of the injection zone. Figure 17 and 18 show the incorporated permeability multiplier in the X and Z directions. If the fracture height exceeds the value used, the actual multipliers would be higher, but this representation is still valid.

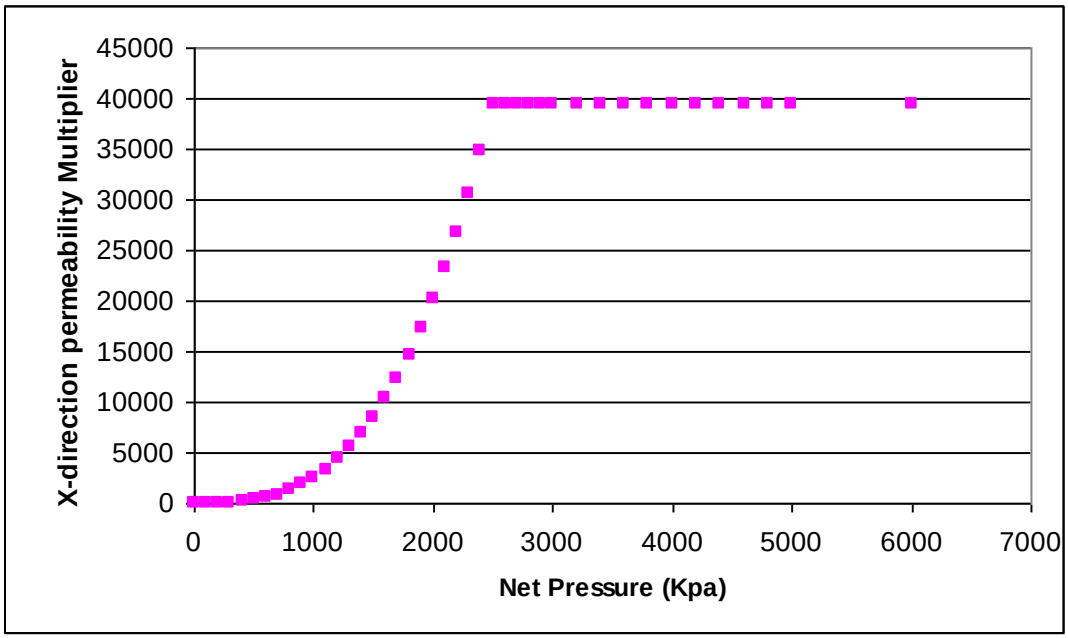

Figure 17: x-Direction permeability multiplier as a function of net pressure.

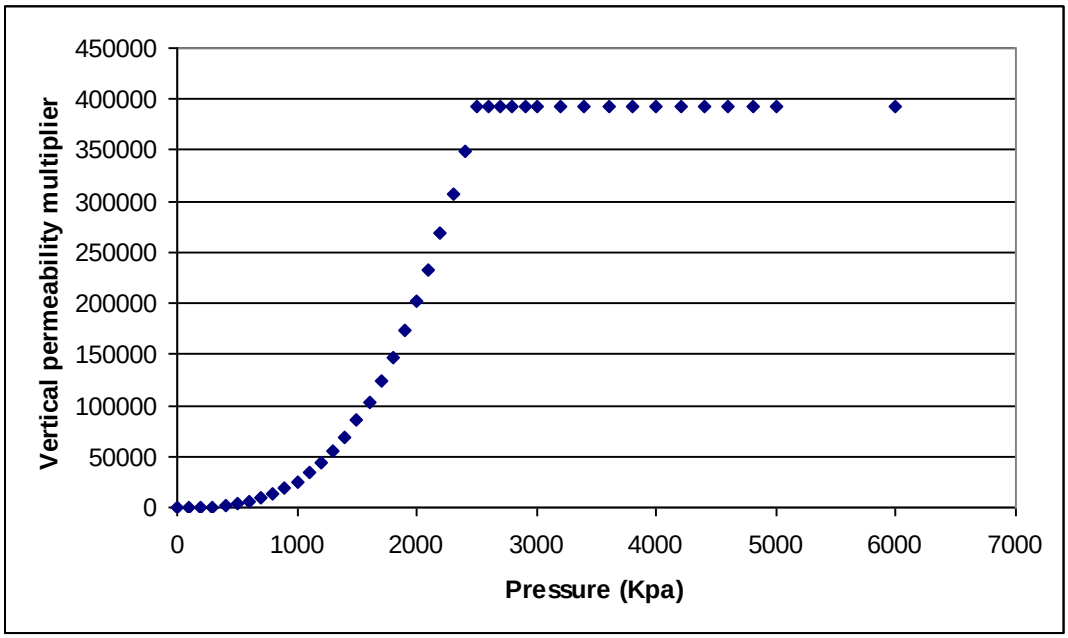

Figure 18: Vertical permeability multiplier as a function of pressure.

5.1.2 Porosity Multiplier

Once the fracture initiates in the formation and starts to propagate, the volume of the fracture will contribute to the porosity of the computational block. This can be accounted for by changing the porosity of the formation rock as a function of pressure in a fashion analogous to the transmissibilities. As a result, the compressibility in the fractured blocks will also change. This effect can be important for the calculation of the maximum volume of CO_2 which can be injected in the reservoir. Therefore a porosity multiplier as a function of net fracture pressure is introduced in the model to account for the added compressibility. The porosity function based on the same fracture parameters is shown in Figure 19.

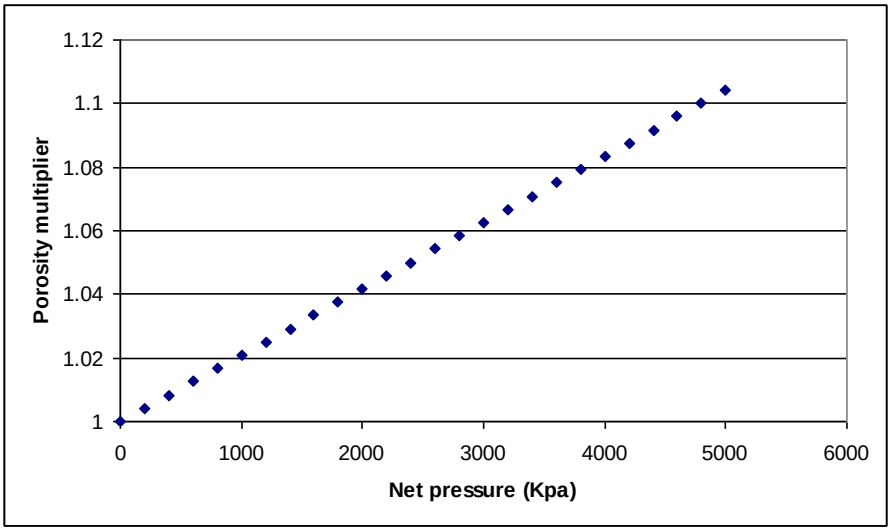

Figure 19: Incorporated porosity multiplier function.

5.2. Results of Injection at 2 Mton/yr Allowing Fracture Propagation

After 50 years of CO_2 injection above the fracture pressure of 2 Mt/yr, a total volume of 100 Mt would be injected into Nisku in 50 years. Figure 20 shows the vertical displacement at surface at the end of injection. Since the injection rate is higher than in the non-fractured case, the displacements are also bigger in the fractured case.

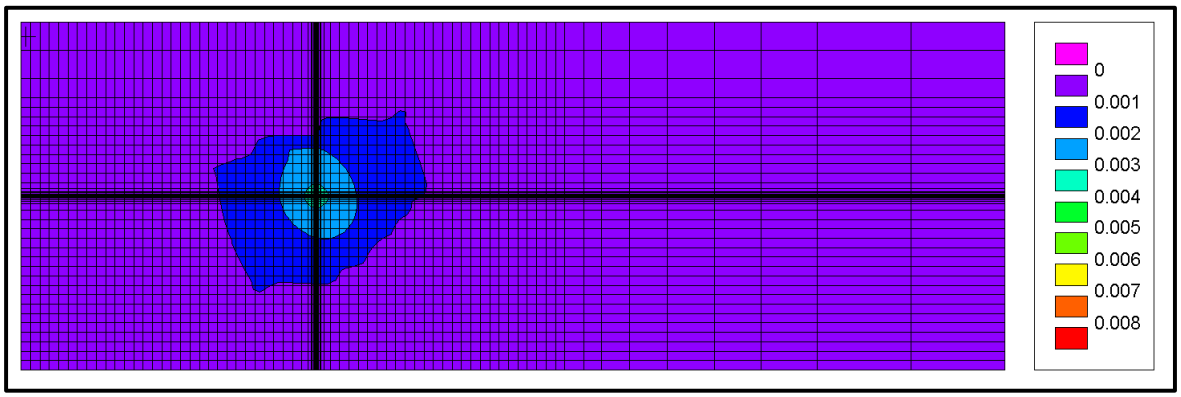

Figure 20: Vertical surface displacement (metre) after 50 years of isothermal CO_2 injection of 2Mton/yr allowing fracture initiation and propagation in the Nisku aquifer.

Figure 21 shows the gas saturation at well block cross section after 50 years of injection. Since there is no stress barrier in the caprock, once the pressure develops in the caprock layer resulting in a negative minimum effective stress, fracture propagation starts in that layer. Figure 22 illustrates a magnified picture of gas saturation for the fractured case after 50 years of injection at the same cross section as in Figure 21.

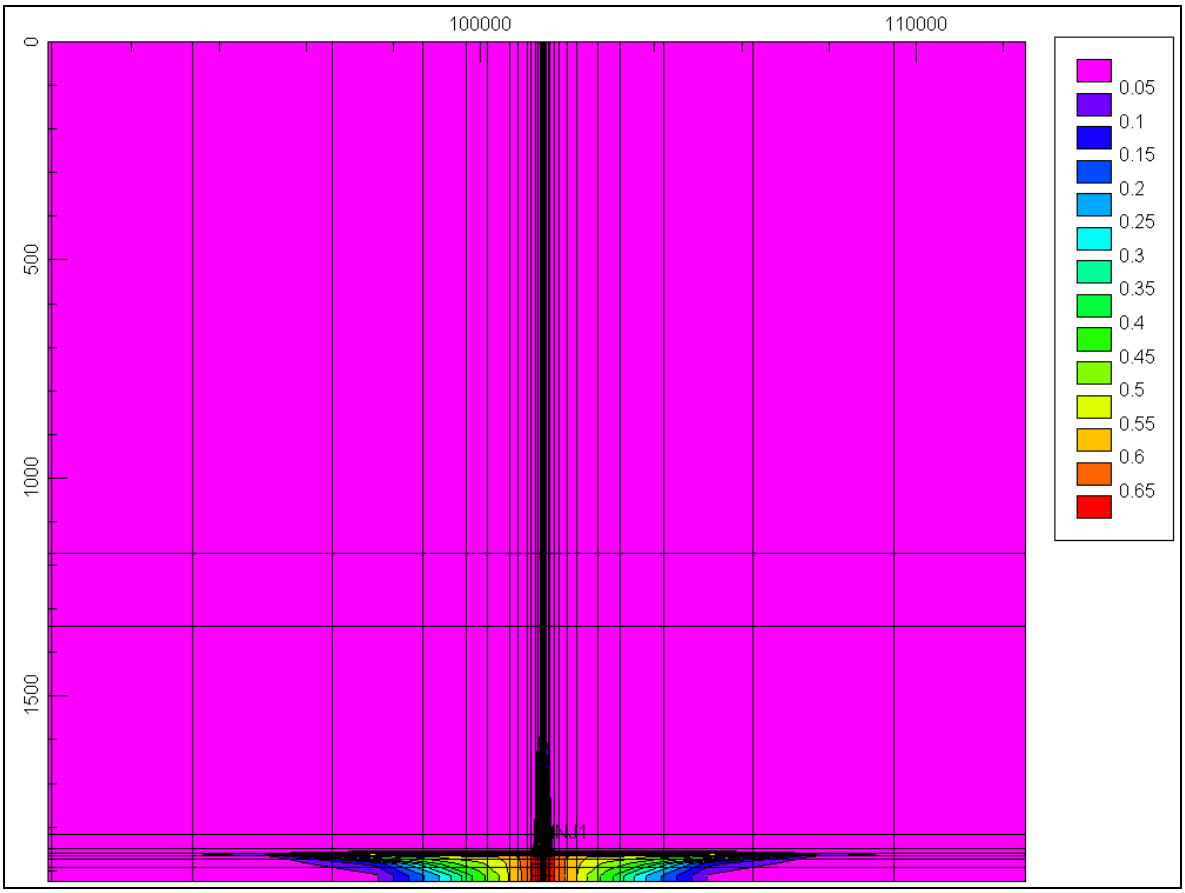

Figure 21: Gas saturation after 50 years of isothermal CO_2 injection at 2Mton/yr allowing fracture initiation and propagation.

The fracture half-length and full height for the isothermal model after 20 years of injection is 27 m and 80 m, and after 50 years of injection reaches approximately 140 m and 112 m, respectively. The fracture growth increases in the late stages due to overall pressurization of the Nisku aquifer, but the CO_2 plume extends well beyond the fracture. It should be noted that due to large computing requirements of the coupled model (runs taking several days), it was not possible to have enough refinement in the 3rd caprock layer, and, as a result, the fracture vertical growth in this layer is over estimated. In addition, the model did not include underburden layers below the Nisku aquifer. More resolution is needed to estimate the fracture height growth accurately. It is important to realize that there are other fracture mechanisms which are not considered in this study and might change the fracture propagation through caprock (Sneddon et al., 1969, Economides and Nolte, 2000, Settari, 1988).

The vertical fracture growth in the isothermal case is sensitive to caprock permeability. We observed that when the caprock permeability is increased, the vertical fracture grows higher into the

caprock. However since the realistic model will include thermal effects (presented in section 6), the effect of caprock permeability is not discussed here but is considered in thermal models.

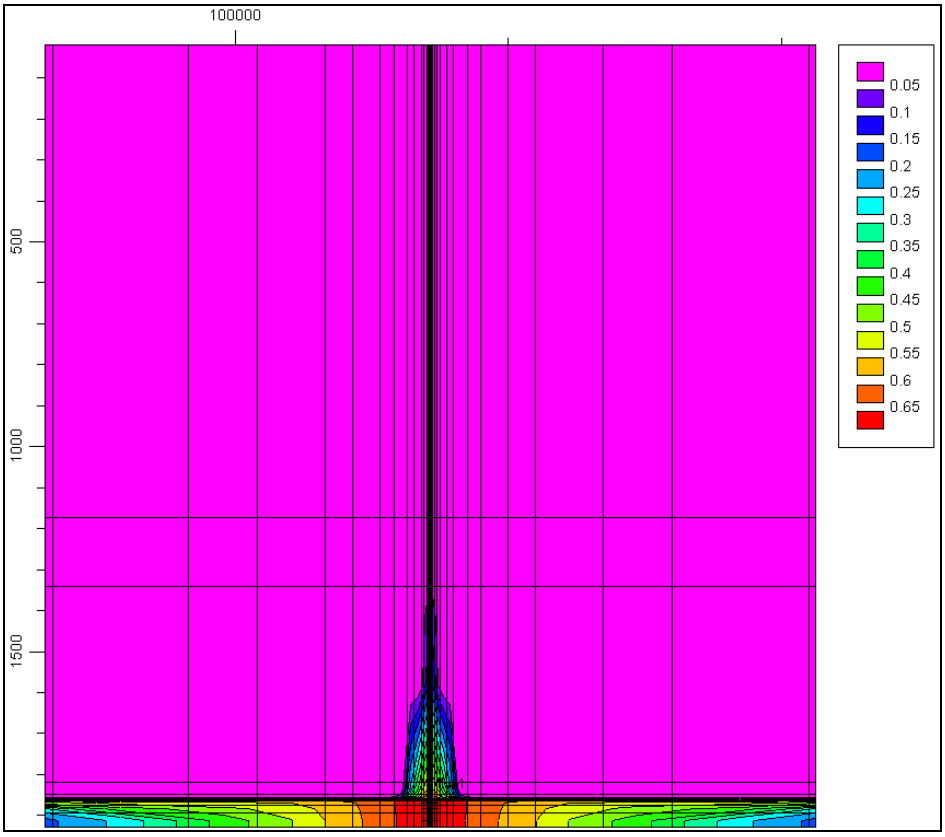

Figure 22: Magnified picture of gas saturation after 50 years of isothermal CO_2 injection of 2Mton/yr allowing fracture initiation and propagation.

6. THERMAL EFFECTS

Since cold CO_2 (at approximately 30 deg C) will likely be injected into the relatively hot Nisku formation (at 60 deg C), thermal effects of injection should be included in the model. Cooling of the formation reduces the total stresses and therefore lowers the fracture propagation pressure. This reduces the pressure differential available for injection, and therefore injectivity. In the case of injection at fracturing conditions, the fracture propagation pressure will decrease and, if the same injection rate is used, this will accelerate fracture propagation.

The isothermal model was extended to include thermal effects of injection. The thermal data used are listed in table 3.(Clauser *and Huenges.*, 1995; Côté *and Konrad.*, 2005)

Table 3: Thermal properties of fluid and rock.

	Rock	Water	CO_2
Thermal Expansion Coefficient (1/K)	1.5E-5	2.6E-4	-
Heat Capacity(Kj/Kg K)	1.2	4.187	0.84
Thermal Conductivity(Kj/m C Day)	165	-	-

6.1. Thermal Effects for Injection Below Fracturing Pressure

We first consider the case of injection below fracturing pressure, described previously. Figure 23 shows the stress and pressure history of both the thermal and isothermal model.

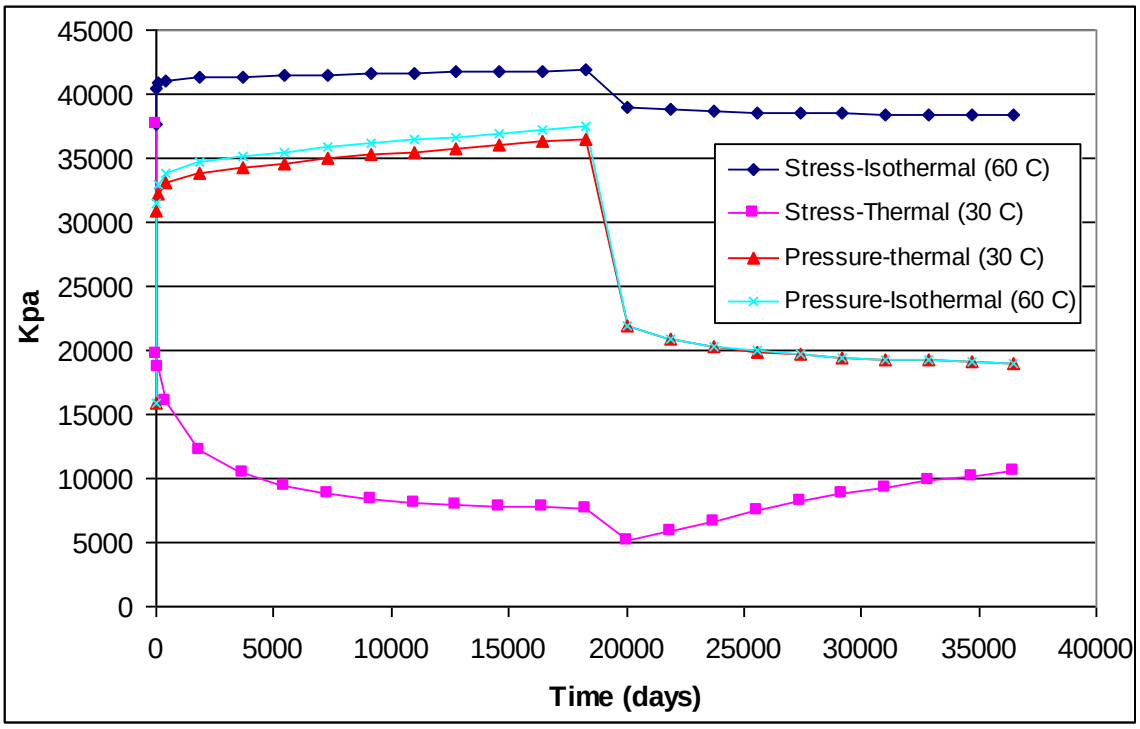

Figure 23: Minimum stress and pressure history for thermal and isothermal model, in the case of injection of 1Mton/yr below fracture pressure.

The reason for this pressure difference is that in the thermal model the injection is modelled at 30 Deg C as opposed to 60 Deg C in the isothermal model. Since the total injected mass of CO_2 is the same for both models and because CO_2 will occupy less volume at 30 Deg C, the pressure will be slightly smaller in the thermal model.

The reduction of stresses in the thermal model is related to the inclusion of temperature effects in the calculation of stresses. After injection stops and temperature rises, stresses will increase again. It should be noted that in the thermal model, the minimum horizontal stress falls below injection pressure at early injection time and creates negative effective stress and therefore would initiate fracture in the formation. It is important to realize that the stress magnitudes after fracturing are not valid in this figure because fracture propagation is not allowed in this model.

Figure 24 shows the surface displacement for thermal and isothermal model. Once the thermal effects in Nisku have influenced a relatively large area around the wellbore, the reduction in Nisku's stress will be transferred to the surface and the surface displacement for the thermal model will fall below that of the isothermal model.

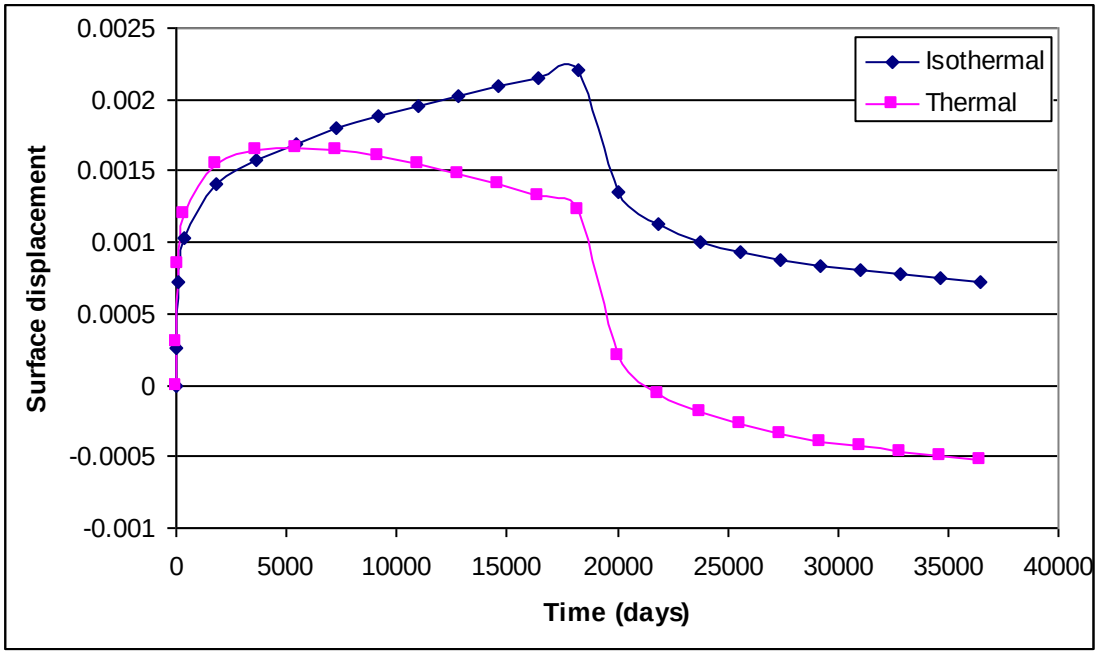

Figure 24: Surface displacement for thermal and isothermal model, for the case of injection of 1Mton/yr below fracture pressure.

6.2. Thermal Effects on Dynamic Fracturing

Including the thermal effects in the dynamic fracture model, there are two important aspects to study:

- Thermal effects on fracture length and vertical growth
- Thermal effects on fracture propagation pressure

In order to study the thermal effects on fracture length and height, the previously described fracture model (Section 5.1) was extended to include the thermal effects of injection. Figure 25 shows the gas saturation at wellbore cross section. This Figure has the same scale as Figure 21.

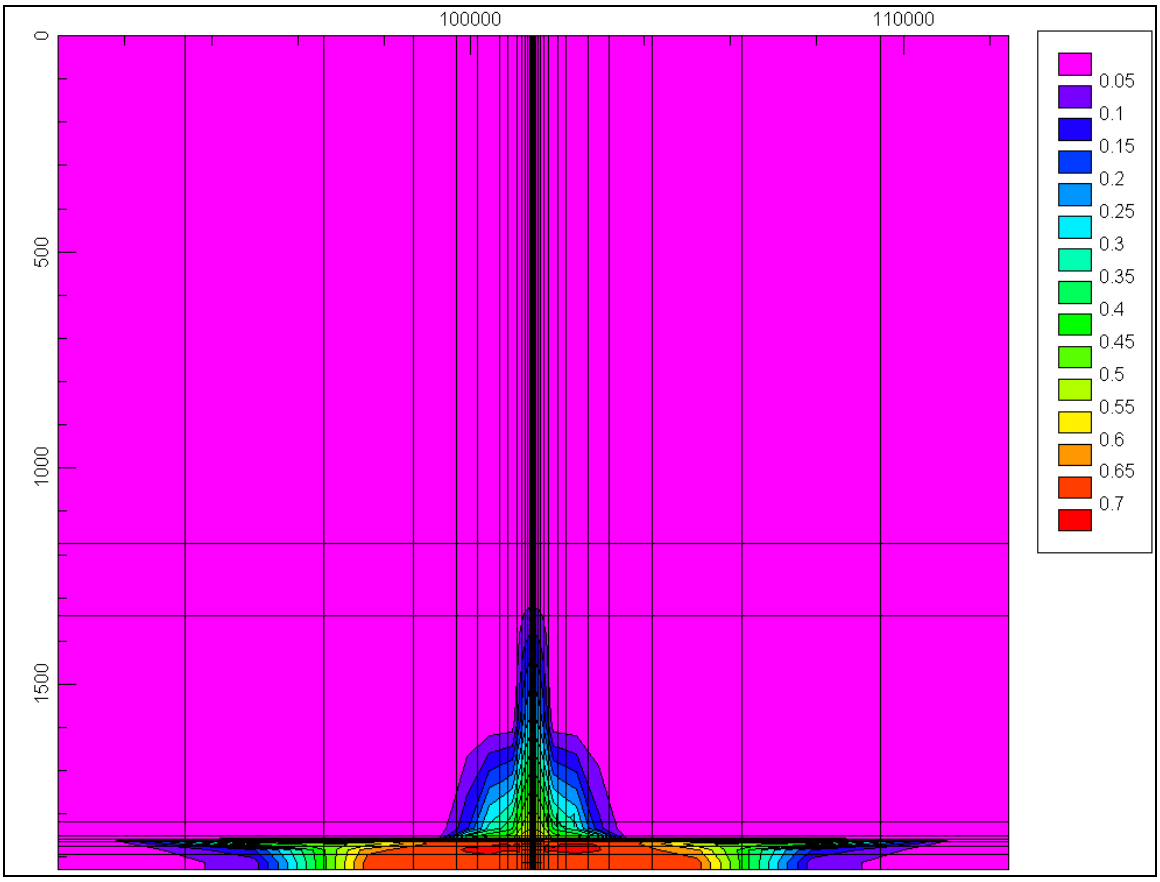

Figure 25: Gas saturation at well block cross section for thermal model.

The dynamics of the fracture propagation is complex as it depends on both poroelastic and thermal effects on stresses. In particular, the vertical growth in the thermal case is different compared to the isothermal one. At early times, since the fracture grows faster in the reservoir layer for the thermal model (due to reduction in temperature), there would be a larger volume of fluid flow into the caprock and the pressurization of the caprock will be higher for the thermal model (fracture permeability effect). However once the temperature change in the caprock starts to help reduce the effective stress to negative values and initiate fracture in the caprock, there would be less pressure drop between the caprock and the aquifer layer (compared to the isothermal case) and, therefore, there would be less fluid flow to the caprock (pressure drop effect), resulting in smaller vertical propagation. We note that limited fracture growth into the caprock is not necessarily harmful. Only if the fracture would grow completely through the caprock, then it would serve as a fluid source for the overlying geological layers.

The thermal effects will help reduce the minimum effective stress and therefore the fracturing pressure. This will result in a smaller pressure drop between the fracture pressure and far-field reservoir pressure for the thermal case compared to the isothermal case. The fracture half-length and height in the thermal case at 20 years are 2700 m and 80 m, respectively, which is larger compared to the isothermal case. After 50 years of injection, the half-length remains constant but the fracture height reaches approximately 112 m. As shown in Figure 25, the gas saturation zone is also larger in comparison to the isothermal case shown in Figure 21a. Due to the dominance of thermal effects, the fracture dimensions are relatively independent of caprock permeability.

Figure 26 shows the fracture propagation pressure for the thermal and isothermal model. As expected since the thermal effects help reduce the effective stress, the fracture propagates at much lower pressure in the presence of thermal effects. This is an important result, because the injection temperature of CO_2 can be controlled at the surface and it can be therefore one of the optimization variables.

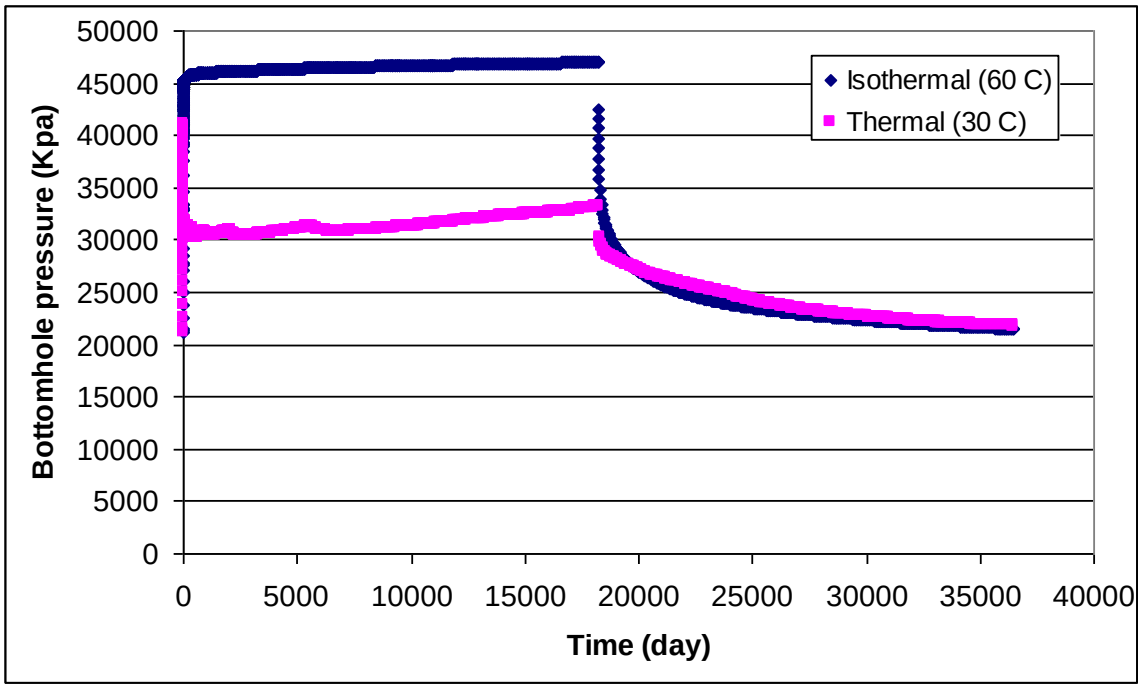

Figure 26: Comparison of fracture propagation pressure for isothermal and thermal model.

7. CONCLUSIONS

1. Injection in the Nisku aquifer (below or at fracture pressure) is not likely to cause any significant surface heave and is not likely to have any environmental impact associated with surface deformations. Surface deformation data can be used in conjunction with seismic measurements to solve an inverse problem for mechanical properties of Nisku and overlying layers. It also can help to plan for the location of the instrumentation and surface monitoring.
2. Injection above the fracture pressure will have the potential to increase the well injectivity but also the possibility of fracturing the caprock. The degree of vertical propagation will strongly depend on the caprock stress state and mechanical properties.
3. Thermal effects of cold CO_2 injection will reduce the fracture pressure and enhance the horizontal fracture propagation through caprock. However, the results of simulation of vertical propagation have been obtained under the most unfavourable assumption of constant minimum stress gradient and are only preliminary (and likely pessimistic).

8. RECOMMENDATIONS

1. One of the main concerns in building a geomechanical model is to avoid the effects of boundaries on the solution. The geomechanical model developed in this study did not include any geomechanical layers below the flow model at its bottom end due to the already large size of the model. It is recommended to extend the geomechanical model to include added layers at the bottom end of the model to eliminate this boundary effect.
2. As mentioned in the Conclusions, the fracture propagation strongly depends on caprock's stress condition. A small stress barrier (i.e., higher stresses in caprock compared to reservoir layer) can prevent fracture from propagating through the caprock layers. Since caprocks commonly act as stress barriers due to their higher Poisson's ratio, it is recommended to study the fracture propagation in the presence of higher stresses in the caprock.
3. After 50 years of CO_2 injection above the fracture pressure in Nisku aquifer, the reservoir pressure will rise from the original value of 16 Mpa and fracture length and height will constantly increase. However if it would be possible to connect the Nisku aquifer and the overlying Wabamun Group, water will start to flow to the latter and the pressure rise in the Nisku aquifer would be smaller and therefore it would be likely that this pressure maintenance scenario would prevent fracture from propagating through the Calmar caprock.
4. Drilling a pilot well and well testing can provide a data source for model validation and to measure flow properties. The following well test plan is proposed for this purpose:
   A) Start the well with a small injection rate and perform a fall off test and measure the Nisku rock properties
   B) Increase the injection rate and perform a step rate test to measure the value of minimum horizontal stress
   C) Inject with higher injection rate to initiate a fracture and use micro-seismic to measure the extent of the fracture.
5. Thermal effects of injection will enhance the fracture propagation. The CO_2 injection stream which comes from the power plant has already been cooled and compressed for increasing injection efficiency. Due to the large extent of thermal effects, it is recommended to control the injection temperature and use the saved compression energy of the power plant to inject lower density CO_2 in order to avoid fracture propagation through the caprock.
6. Experimental results on compressibility and thermal expansion coefficient of rock were received at the time when the geomechanical simulation was already completed. The reported values for these two properties are 1-2 orders of magnitude different from what was used before in geomechanical models. This difference could make a noticeable difference in injectivity and thermal effects of injection. It is recommended to update the flow and geomechanical models based on the new reported properties.

9. REFERENCES

Bennion, B., Bachu, S., (2005), "Relative Permeability Characteristics for Supercritical CO_2 Displacing Water in a Variety of Potential Sequestration Zones in the Western Canada Sedimentary Basin", SPE 95547.

Clauser, C., Huenges, E., (1995), "Thermal Conductivity of Rocks and Minerals", American Geophysical Union.

Côté, J., Konrad, J.-M., (2005), "Thermal conductivity of base-course materials", Canadian Geotechnical Journal 42: 61–78.

Economides, M.J. and Nolte, K.G. (editors) (2000). *Reservoir Stimulation*, John Wiley and Sons, 2000.

Hassanzadeh, H., Pooladi-Darvish, M., Elsharkawy, A.M., Keith, D.W. and Leonenko, Y., (2007), "Predicting PVT data for CO_2-brine mixtures for black-oil simulation of CO_2 geological storage", International Journal of Greenhouse Gas Control.

Hitchon, B., (1996), "Aquifer Disposal of Carbon Dioxide, Hydrodynamic and Minernal Trapping - Proof of Concept". Sherwood Park, Geoscience Publishing Ltd.**:P.** 58.

Keith, D., Lavoie, R., (2008), "Wabamun Area CO_2 Sequestration Project (WASP)", Project Overview.

Michael, K., Bachu, S., Buschkuehle, M., Haug, K., and S. Talman. in press. Comprehensive Characterization of a Potential Site for CO_2 Geological Storage in Central Alberta, Canada, AAGP Special Publication on Carbon Dioxide Sequestration.

Bell, S.J. and Bachu, S., (2003), "In-situ stress magnitude and orientation estimates for

Cretaceous coal-bearing strata beneath the plains area of central and southern Alberta:Bulletin of Canadian Petroleum Geology", v. 51, p. 1–28.

Mossop, G., Shetsen, I., "Geological Atlas of the Western Canadian Sedimentary Basin", Chapter 12, P. 191, Devonian Woodbend-Winterburn Strata, Copyright 1994, Canadian Society of Petroleum Geologists, Alberta Research Counsel, ISBN: 0-920230-53-9.

Quintessa, National Institute of Advanced Industrial Science and Technology of Japan, Quintessa Japan, JGC Corporation, Mizuho Information and Research Institute, (2007), "Building Confidence in Geological Storage of Carbon Dioxide" Ministry of Economy, Trade and Industry (METI), IEA Greenhouse Gas R&D Programme (IEA GHG).

Settari, A., (1988), "Quantitative Analysis of Factors Influencing Vertical and Lateral Fracture Growth", SPE Prod. Eng. (Aug. 1988), pp. 310-322.

Sneddon, I. N. and Lowengrub, M. (1969).*Crack Problems in the Classical Theory of Elasticity*, John Wiley & Sons Inc., New York, 1969.

Zoback, M.D., (2007), Reservoir Geomechanics, Cambridge University Press, Cambridge, 449 p.

Perkins, T.K. and Kern, L.R., "Widths of hydraulic fractures", Journal of Petroleum Technology, Sept. 1961, Vol, 13, No.9, 937–949.